50h 3AF International Conference
on Applied Aerodynamics
29-30 March – 01 April 2015, Toulouse - France

FP67-2015-Benard

Experimental Optimization by Genetic Algorithm for Flow Separation Control with Surface Plasma Actuator

N. Benard[(1)] , J. Pons-Prats[(2)], J. Periaux[(2),(3)], G. Bugeda[(2),(3)], J.P. Bonnet[(1)] , and E. Moreau[(1)]

[(1)] Institut PPRIME UPR3346, Bat H2 SP2MI Bld Marie et Pierre Curie 86960 Futuroscope, France, Email: nicolas.benard@univ-poitiers.fr
[(2)] International Center for Numerical Methods in Engineering (CIMNE), c/ Esteve Terrades 5 08860 Castelldefels, Spain
[(3)] Universitat Politècnica de Catalunya (UPC), c/ Gran Capità s/n 08034 Barcelona, Spain

ABSTRACT

The present investigation concerns the active control of a turbulent separated flow downstream of a backward-facing step by surface plasma discharge. A single-objective genetic algorithm is implemented in order to achieve the minimization of the recirculation length. For that purpose, a series of unsteady pressure sensors installed on the bottom wall can detect the mean reattachment location. The optimized variables are the voltage amplitude, burst frequency and duty-cycle of the applied signal. Here, single-objective evolutionary algorithm, usually coupled to computational fluid dynamics simulation, is coupled with real-time experimental data for the first time. It is shown that the genetic algorithm is successful at finding the optimum forcing conditions for a turbulent flow at Re_h=30000 (Re_θ=1650). Then the optimal conditions are explored by time-resolved PIV in order to give physical explanations of the best input signal identified from the evolutionary algorithm. In particular, the present investigation confirms that minimization of the recirculation is achieved by forcing the flow periodically at the shear layer mode of instability. For this type of forcing, the shear layer evolution is strongly modified with a deep regularization of the vortical flow structures and the triggering of vortex pairing mechanism both promoting a shortened recirculation caused by enhanced turbulent momentum transfers.

1. INTRODUCTION

Among several applications, optimization by combining evolutionary algorithms and numerical simulations has demonstrated their potential to solve high dimensional problems. In a few contributions, evolutionary algorithms are used to optimize the flow control conditions by full numerical approaches. For instance, suction/blowing jet mounted on the upper surface of a NACA0012 airfoil has been numerically optimized in [1]. The optimal forcing mode and more specifically the forcing frequency that maximize the spreading rate of a turbulent jet has been shown in [2] by direct numerical simulation. The problem of time-averaged drag minimization of a circular cylinder by rotary oscillation has been addressed in [3]. Recently, a NSGA-II code has been numerically applied to optimize the flow reattachment along a NACA0015 model by plasma discharge [4]. In the present study, because genetic algorithm only requires the evaluation of the cost function regarding a set of control parameters, such an evolutionary algorithm is used in conjunction with experimental measurements in a feedback loop process.

The present investigation concerns a fundamental configuration: the turbulent flow separation downstream of a Backward-Facing Step (BFS). This configuration is well-adapted for defining unsteady flow control approaches because the flow behind a BFS presents a large variety of

periodic motions while the location of the separation point is known and stable [5, 6, 7]. The BFS configuration is a rich environment in terms of periodic motions and it offers a lot of flow control scenarios even for actuators producing a low momentum transfer such are surface plasma discharges [8]. Plasma actuators have been used in a lot of aerodynamic flow configurations but among them, BFS has only received a recent attention. For instance, the effectiveness of DBD actuator to shorten the recirculation bubble (-35%) at low Reynolds number and laminar regime has been shown in D'Adamo et al. [9] by forcing the flow with a vertical plasma jet. Studies at a higher Reynolds number (Re_h~30000) have been recently published. In [10], a reduction in the recirculation length of about 20% is observed for unsteady actuation at the step mode of instability (St_h~0.25). The unsteady wall pressure signals suggested a strong periodization of the flow structures caused by the imposed periodic fluctuations.

This article presents an experiment approach using non-thermal plasma in conjunction with a genetic algorithm. The genetic algorithm is used to solve a single-objective optimization problem (minimization of the reattachment location) with varying voltage amplitude, burst frequency and duty-cycle. In a second part of the paper are introduced time-resolved flow measurements by PIV with the goal to interpret the best forcing conditions determined by the numerical optimizer.

2. EXPERIMENTAL SETUP

The model includes a ramp, followed by a flat plate and ended by a backward step having a height, h, of 30 mm and a spanwise length of 300 mm. This model is installed in a closed-loop wind-tunnel (Figure 1) having a moderate turbulent intensity (1%). The dimension of the test section is 300x300x1000 mm^3. The model covers the full spanwise of the test section and the expansion ratio equals to 1.1. The aspect ratio (channel width on step height) is larger than 10 this guaranteeing for a two-dimensional flow in the center of the wind tunnel. All measurements are performed for a free-stream velocity of 15.6 m/s. The study is performed for a fully turbulent flow with tripped boundary layer and Reynolds number Re_h of 30000. Preliminary measurements by LDV have shown that the boundary layer at the step corner presents a shape factor of 1.6, a momentum thickness of 1.63 mm and a displacement thickness of 2.62 mm.

Figure 1: Closed-loop wind-tunnel for backward facing step experiments.

The actuator is made of two strips of black aluminum tape glued asymmetrically on both sides of a 3-mm thick dielectric (the model in PMMA serves as dielectric barrier). The electrode arrangement is defined to produce a wall jet tangentially to the step in the positive x direction (Figure 2). Due to the confined environment and a desire to have a direct interaction between the plasma discharge and the flow separation at the step corner, the electrode arrangement is not optimized to reach maximum induced velocity.

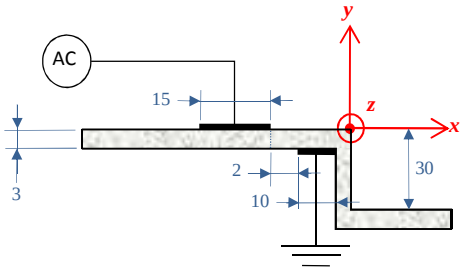

Figure 2: Sketch of the model equipped with a single linear DBD plasma actuator and coordinate system

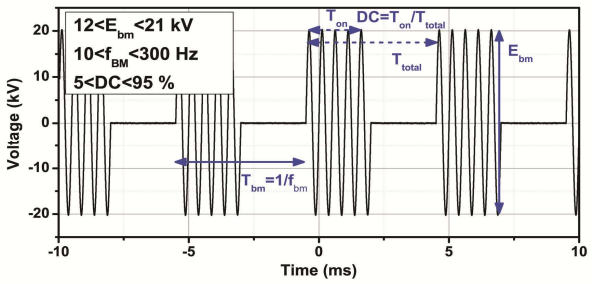

Figure 3: Applied waveform and identification of the three design variables of the optimization problem.

The actuator is then a Dielectric Barrier Discharge (DBD) plasma actuator, a discharge well-known to produce a thin wall jet due to the electrohydrodynamic body force caused by the momentum exchanges between neutral and charged particles colliding in a weakly-ionized environment [8]. Here the applied voltage is between 12 and 21 kV in amplitude while the driving AC frequency is 2000 Hz. In order to reach a frequency range for which the flow is receptive, the input signal is modulated by burst with variable

duty-cycle. The low voltage electrical signal is produced by a generator card (PXI-5402), this low voltage being amplified with a scale factor of 3/3000 V (Trek 30/40) before supplying the top electrode. The parameters space of the optimization problem concern the voltage amplitude, the burst frequency and the duty-cycle (Figure 3). In the present investigation the maximum velocity produced by the discharge does not exceed 4 m/s (velocity ratio U_{DBD}/U_0=0.26).

The bottom part of the step model is equipped with 32 unsteady wall pressure sensors in its central plane. These sensors are based on piezoelectric technology and they have a bandwidth of 2 kHz for a max pressure of 250 Pa. The output voltage signals of the pressure sensors are recorded by PXI hardware (2.16 GHz dual core) with 32 channels acquisition card (PXI-6259). A LabVIEW code couples the acquisition and generator cards. The measures consist in recording the pressure fluctuation amplitudes at each sensor location and in computing the wall pressure fluctuation coefficients $C_{P'}$. Then, the mean reattachment point is estimated by the position of the pressure fluctuation peak along the stream wise direction on the wall as indicated in literature [11]. Due to the highly unsteady flow reattachment, a converged estimation of the reattachment point requires 5 seconds of continuous recording. An illustration of the $C_{P'}$ distribution along the bottom wall is proposed in Figure 4. The LabVIEW code is designed to autonomously determine the reattachment location. The error in the X_R evaluation is ±0.15h, the spatial resolution of the wall sensors.

The purpose of this study is an experimental minimization of the reattachment location by wall pressure measurements. To gain insight into the

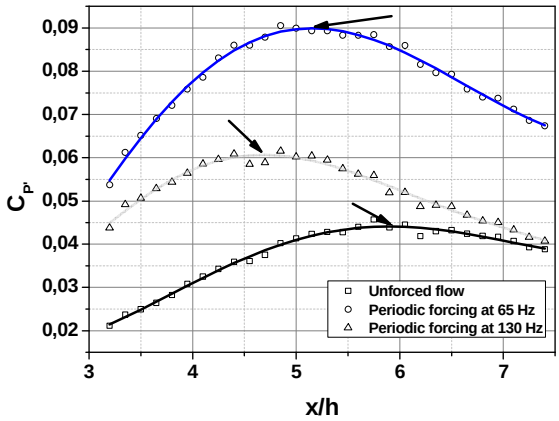

Figure 4: Illustration of the pressure fluctuation coefficients in the streamwise direction for natural and controlled flows. The black arrows correspond to the estimated reattachment locations.

modification of the flow dynamic when optimized control is applied, the wall pressure measurements are completed by time-resolved particle image velocimetry acquisitions for the natural and controlled flows. In the latter case, the optimized electrical signal is applied to the plasma actuator. The PIV system is composed by a high-speed camera (Photron, APX-RS), a single head Nd:YLF high-speed laser with dual oscillator (Quantronix, Darwin-Duo), a triggering unit (EG, R&D Vision) and a PC running Davis Lavision software. Measurements are conducted only in the mid-span of the model where the flow is not contaminated by side wall effects. The camera is operated at 2000 full frames per second at 1024x1024 pixels². The two velocity components are computed using a cross-correlation algorithm with adaptative multipass, interrogation windows of 64 x 64 to 16 x

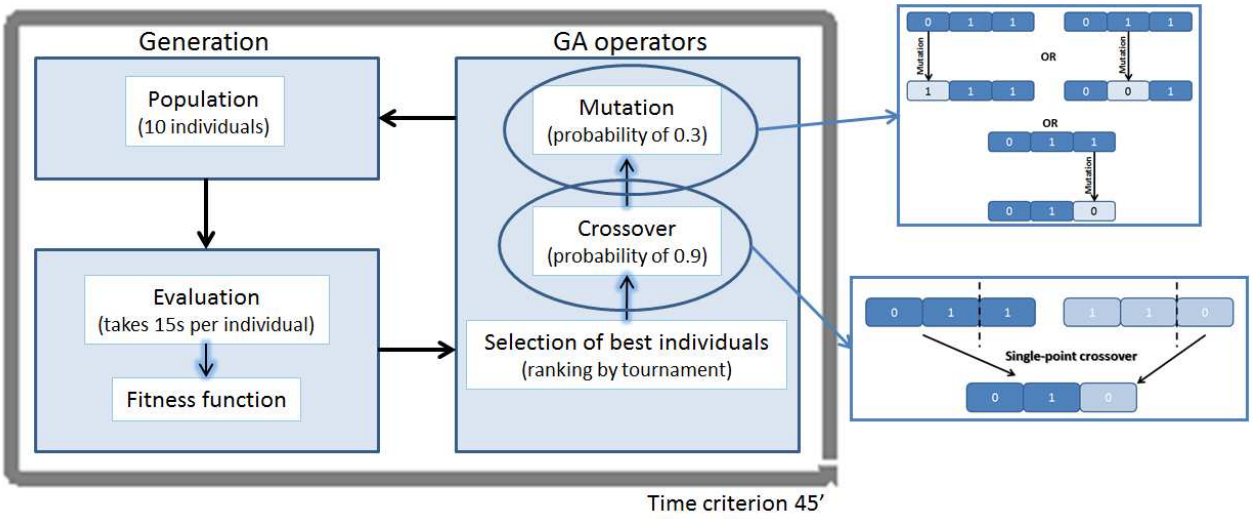

Figure 5: Illustration of the GA procedure for minimization of the flow reattachment location

16 pixels and an overlap set to 50%. This results in a spatial resolution of 4.5 x 4.5 mm² for the vector fields.

3. GENETIC ALGORITHM OPTIMIZER

Optimization methods define a set of tools and techniques that help engineers to solve complex problems optimizing an objective function while fulfilling a set of constraints [12]. This type of problem consists in maximizing or minimizing an objective function f depending on N_x design variables varying over a bounded search space. There are different types of numerical algorithms for the solution of such optimization problem. Among the optimization methods available, the present investigation focuses on genetic algorithm approach, a stochastic method having demonstrated its robustness in complex problems where the objective function f is totally unknown. The solution is a unique or a set of individuals that have been selected by combination of selections, crossovers and mutations.

In the present study, the objective function is the mean reattachment location X_R while the design variables are the voltage amplitude E, the burst frequency f_{BM} and the duty-cycle DC (see Figure 3). The objective is to minimize the function X_R, this function being evaluated by the wall pressure coefficients. The optimization process starts with a randomly generated population (also called generation), including 10 individuals. Each individual (made of the voltage amplitude, burst frequency and duty-cycle) is evaluated by applying the signal command to the plasma discharge. The evaluation of one individual lasts 15 seconds, this time including 5 seconds for achieving a stable control, 5 seconds of data sampling and 5 seconds to let the flow fully relax. Finally, the code computes the wall pressure fluctuation coefficients and it determines the fitness function X_R of the evaluated individual. Then, the operators of the GA are the selection, the crossover and the mutation. The selection operator selects the best performing individuals of each population to enable other operators to produce new offspring. Crossover is taking two selected individuals and it combines them to create a new offspring. Several techniques can be used to determine the point where the genetic information is split to add the genetic information from the second individual. Here, the information from the individuals is combined by

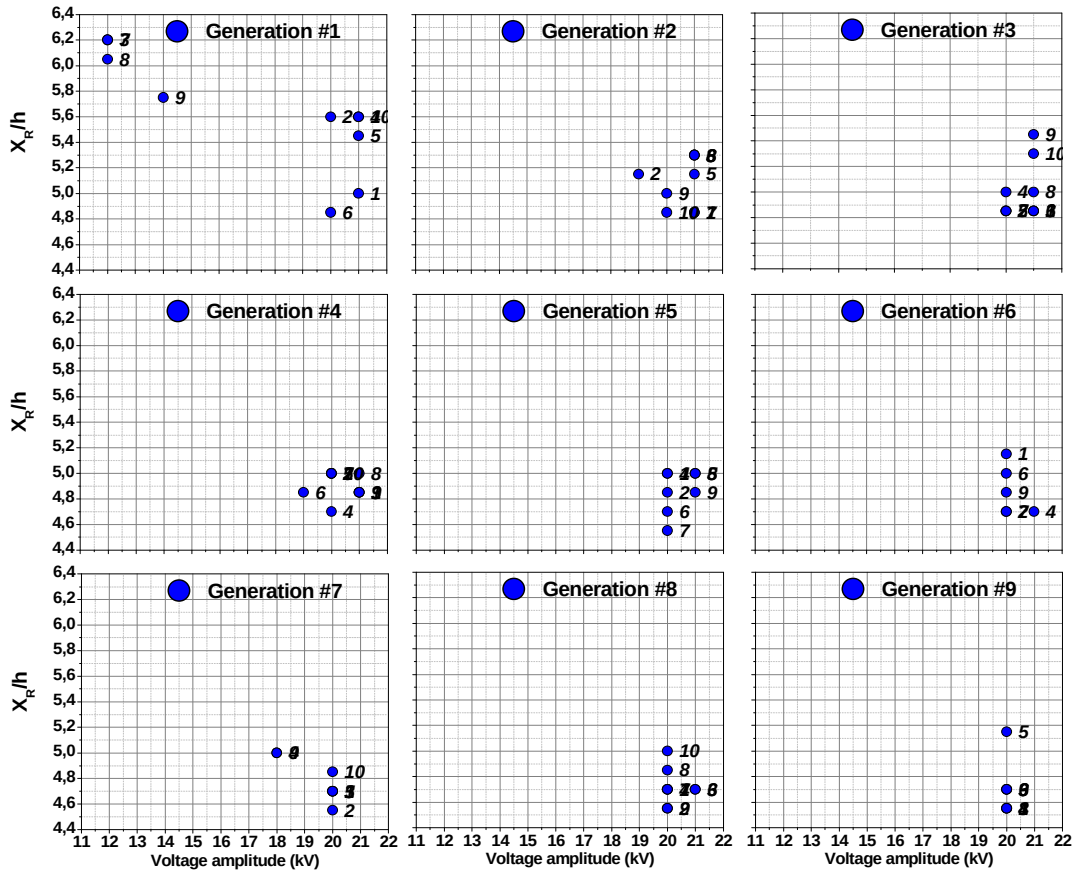

Figure 6: Evolution of the objective function X_R for the first nine generations when the voltage amplitude (design parameter x_1) is varied (numbers relate to the identification number of the individuals).

one-point crossover. Finally, the mutation operator creates new offspring modifying arbitrarily the information contained in one selected parameter of one individual. In this study the individuals are encoded by real-value approach where each individual is represented by a string containing all the data for the input parameters. Operations of selection, cross-over and mutation are applied to these strings over the iterations to generate new individuals, and to evolve them towards the optimum value. The multi-input genetic algorithm automatically stops after 60 min, which means 12 generations of individuals this in order to limit the operating time of the plasma discharge (and avoid damaging the dielectric barrier).
Here, the GA code is a simplified version of multi-objective genetic algorithm module in Robust Multi-objective Optimization Platform (RMOP) developed at CIMNE. Only the subset of tools corresponding to single objective optimization problems has been used but more details of RMOP can be found in references [13].

4. RESULTS

The results are organized in two parts. A first section where the GA code is coupled with the experiments to get the best forcing conditions that minimize the recirculation bubble and a second part in which the mean and time-resolved flow fields are compared for natural and controlled flow conditions.

4.1 Single-objective optimization of the plasma actuation by genetic algorithm

The procedure of coupling experimental sensors and actuators with a numerical optimization code, as an analogic solver, has been briefly introduced in section 3. The minimization of the reattachment length is achieved by inspecting the influence of three design variables (x_1, x_2, x_3):

- x_1: Voltage amplitude (V, in kV); $\mathrm{V} \in \mathbb{N}, 12 \leq \mathrm{V} \leq 21$
- x_2: Burst frequency (f_{bm}, in Hz); $f_{bm} \in \mathbb{N}, 10 \leq f_{bm} \leq 300$
- x_3: Duty-cycle (DC, in %); $\mathrm{DC} \in \mathbb{N}, 5 \leq \mathrm{DC} \leq 95$

To illustrate the GA code process and its convergence, the evaluation of the individuals of different generations are shown in Figure 6, 7 and 8. In these figures is shown the evolution of objective function X_R when the design variables

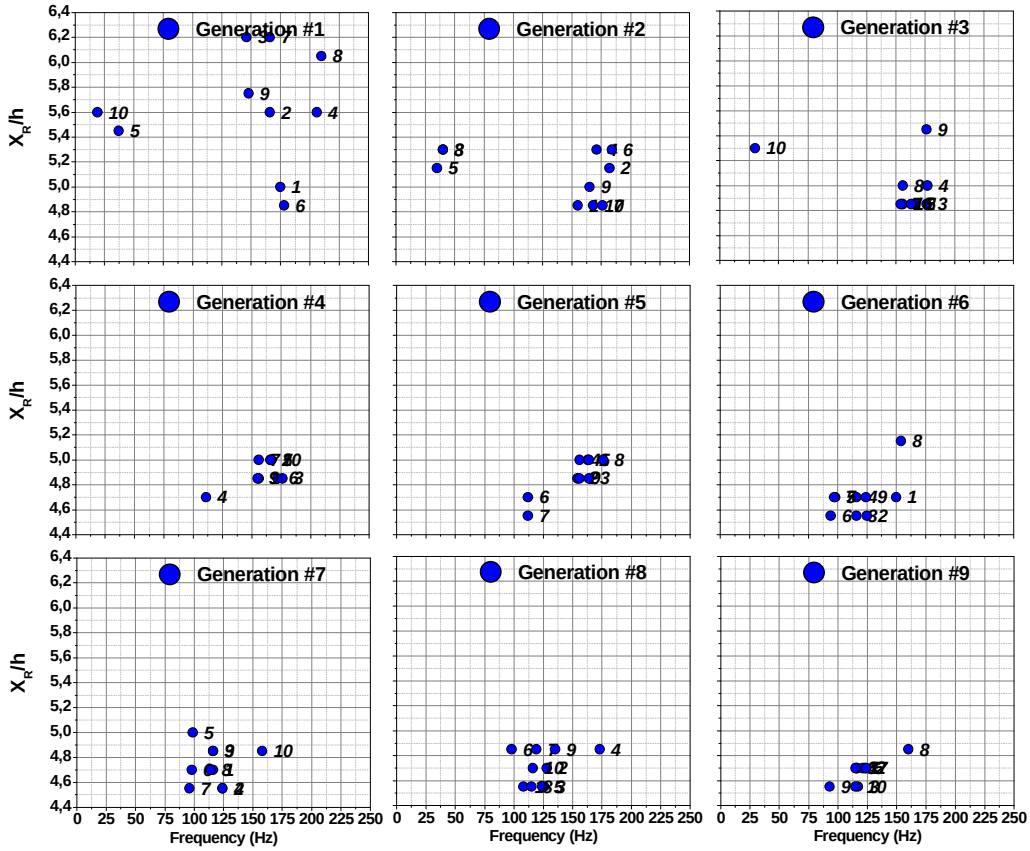

Figure 7: Evolution of the objective function X_R for the first nine generations when the burst frequency (design parameter x_2) is varied (numbers relate to the identification number of the individuals)

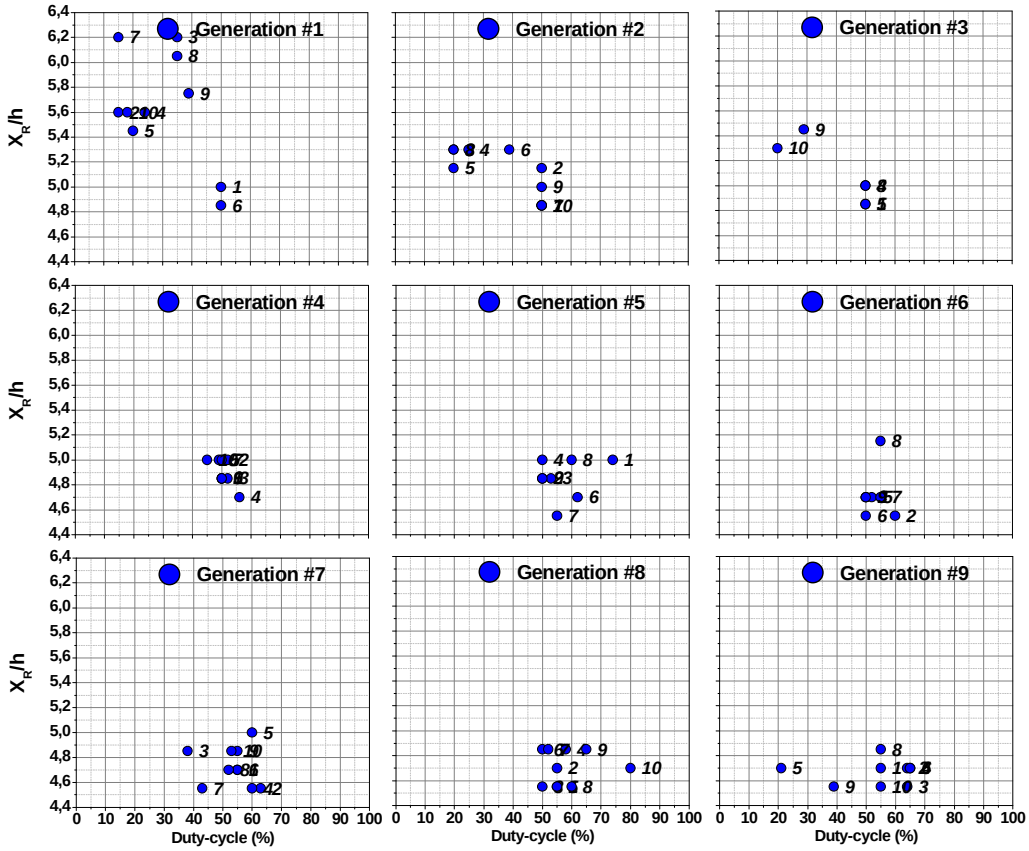

Figure 8: Evolution of the objective function X_R for the first nine generations when the duty-cycle (design parameter x_3) is varied (numbers relate to the identification number of the individuals).

are simultaneously optimized. Since the first generation is randomly defined, the design variables cover the whole search space. As it is shown in Figure 6, the GA approach finds the optimal voltage amplitude in only a few generations. The mean reattachment position varies from 6.2h down to 4.55h. The fast convergence rate is caused by the plasma actuator itself. Indeed, the increase in mean flow velocity produced by the actuator with the voltage amplitude can be fitted by a second order polynomial. Increasing the voltage amplitude has a strong influence on the reduction of the recirculation zone. But too high amplitude promotes a filamentary discharge, a plasma regime less effective to produce EHD effects. This explains the convergence to an optimized value of 20 kV. The evolution of the code optimizing the burst frequency is shown in Figure 7. The convergence rate is lower for this variable. The first three generation converges to values about 175 Hz. In the fourth generation, one of the individual (#4) mutated and it finds a better minimization of X_R. Then, the variable x_2 of the individual converges to a new optimum. The evolution of the duty-cycle is shown in Figure 8. As for the burst frequency, the GA code needs several generations to converge to a duty-cycle between 40 and 70%.

The results for the final generation as well as the convergence of the individuals are plotted in Figure 9. The individuals of this generation correspond to the optimized solutions. For the worst individuals, a mean reattachment at 6.5h has been measured. However, the GA code coupled with the plasma discharge reduces the recirculation by 30%, the reattachment point moving up to 4.55h. The gain in X_R is precisely the one already obtained by an extensive parametric investigation conducted by stereoscopic PIV measurements in [14]. However, here the optimization is performed in one hour when the PIV measurements taken several months of data-processing. The convergence plot confirms that the GA code quickly evolves to the optimized solution. Finally, regarding the design variables, the three parameters that recover the optimal individual are:

- Voltage amplitude of 20 kV
- Burst Frequency of about 125±5 Hz
- Duty-cycle of about 50-80%

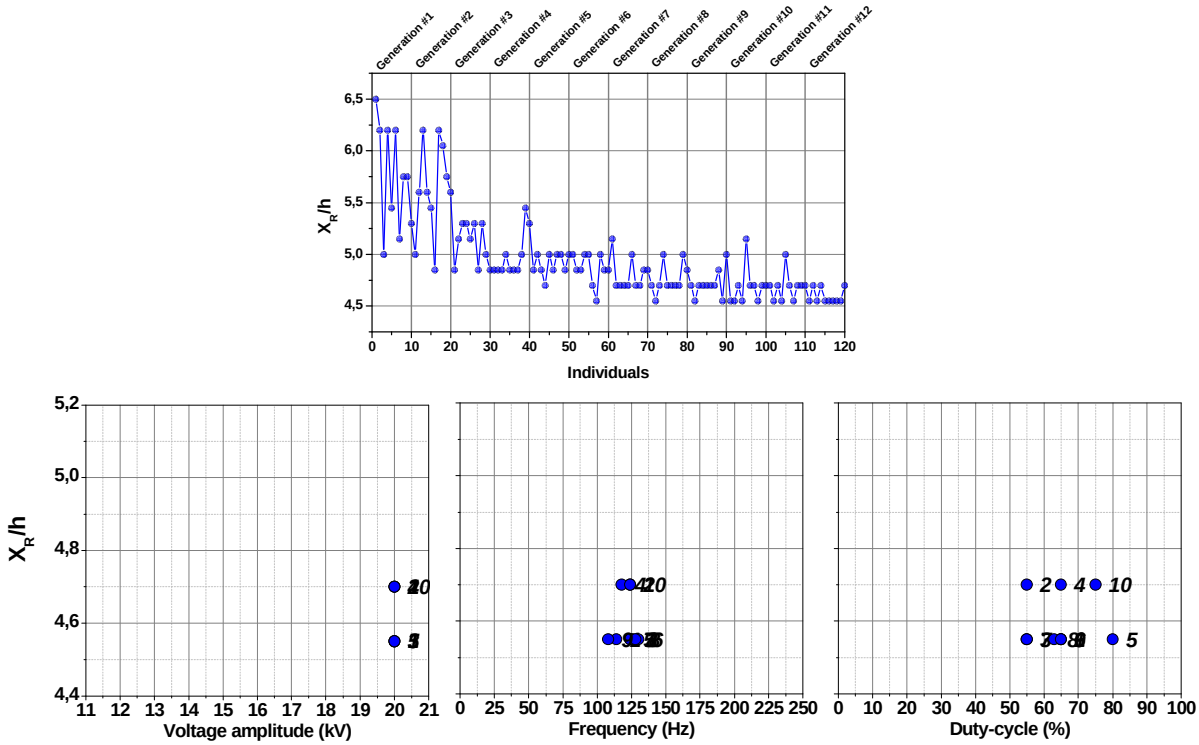

Figure 9: Convergence of the GA optimizer (top) and fitness function of the final generation (#12) according to the voltage amplitude, the burst frequency and the duty-cycle.

The burst frequency of the optimized electrical signal can be scaled on a geometric parameter as the step height or on one of the inlet flow characteristics such as the momentum thickness θ at the step corner. In the present study, the optimized burst frequency corresponds to St_h=0.24 or St_θ=0.013. Forcing the flow by periodic fluctuations at these two Strouhal numbers are well-known, by the flow control community, to minimize the location of the reattachment point. Periodic fluctuations at St_h=0.24 excites the step instability mode as discussed in [11] while a forcing at St_θ=0.013 has a recognized influence on the shear layer mode [5, 15], a convective instability process that can reduce the reattachment by promoting the pairing of the vortical flow structures embedded in the turbulent shear layer [16]. The optimized forcing conditions identified by the GA code are then in full agreement with the literature whether the type of flow control actuator [11, 17].

4.2 Measurements by time-resolved PIV

The GA code has found the best forcing conditions to minimize the reattachment position. In a second step, a PIV experimental campaign has been conducted. The objective focused on the flow characterization of the natural BFS flow and the best forcing condition identified from the GA optimizer.

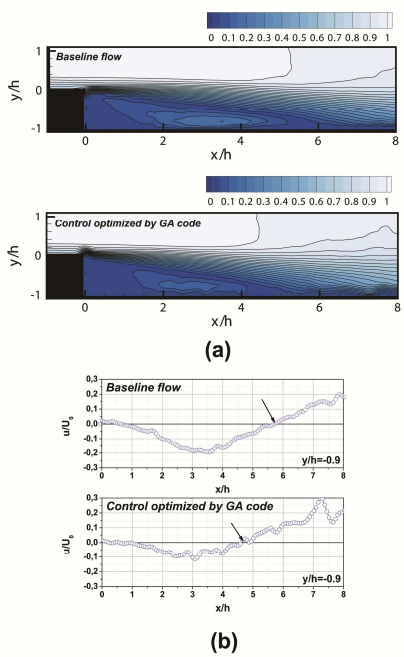

Figure 9: Mean normalized flow field (a) and velocity extraction at y/h=-0.95 (b)

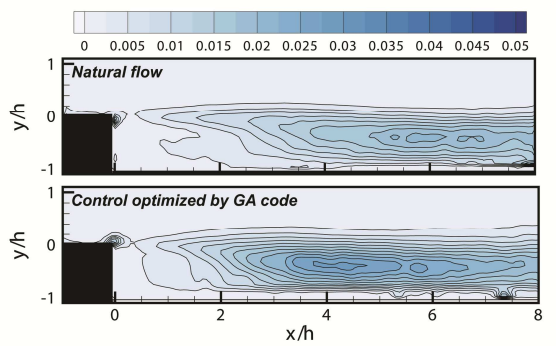

Figure 10: Iso-contours of the normalized turbulent kinetic energy.

The mean flow field computed on 24000 velocity fields is shown in Figure 9a (velocity norm normalized by U_0). The natural flow case as well as the best control parameter defined from the GA code are summarized in this figure (E=20 kV, f_{BM}=125 Hz, DC=50%). Velocity extraction close to the bottom wall are also presented in Figure 9b in order to identify precisely the mean reattachment point by inspecting the change in the u-velocity direction. The actuation clearly conduces to a reduction of the recirculating bubble. The natural flow reattaches at 5.75h downstream of the step wall. This value is in good agreement with the reattachment location extracted from the wall pressure fluctuations distribution (see Figure 4). When the plasma discharge is operated at its optimized parameters, the mean reattachment point is moved further upstream with a location identified at a distance of 4.6h from the step.

The distribution of the Turbulent Kinetic Energy (TKE) is illustrated in Figure 10. The optimized forcing moves the region of high turbulent kinetic energy in the upstream direction. The region of maximum TKE is located at x=4h and a slight deviation of the region of high TKE toward the upper wall of the test section can be noticed around x=3h. A trace of the periodic fluctuations imposed by the discharge can be observed close to the step corner in the region where the discharge propagates.

The effectiveness of a periodic forcing at St_θ =0.013 is further demonstrated by inspecting the evolution of the vorticity thickness with downstream location x/h (Figure 11). For the natural and controlled flows, the vorticity thickness linearly grows with the downstream distance (zone I in Figure 11). The linear region stops at x=3.5h for the natural flow and it is followed by a region where the thickness of the shear layer stabilizes (zone II in Figure 11a). Past the separation point, the vorticity thickness increases again due to the lateral displacement of the reattaching region. With the plasma discharge, the shear layer stops its development at a shortened distance (x=3h) however the thickness still increases up to x=4.5h (zone II), but at a reduced rate than in zone I. This suggests a change in the growing mechanism of the fully developed shear layer as it will be demonstrated later.

The vortical flow structures can be tracked by inspecting the temporal evolution of the velocity fluctuations at several x/h positions (Figure 12). The signature of the structures is an alternation of positive and negative fluctuating velocities. With the downstream distance, the vortical flow structures increase in size and are deflected toward the bottom wall. It is clearly shown in Figure 12 that the control by applying the parameters defined by the GA optimizer reinforces the vortical flow structures. The vertical fluctuating velocities are significantly increased and the train of vortical flow structures has clearly gained in periodicity. At x=4h, the frequency of the vortical trains seems to be reduced by the periodic forcing at the step corner. This corroborates with the change in the growing rate of the vorticity thickness observed in Figure 11. The power density spectra of the fluctuating vertical velocity component are shown in Figure 13. At the beginning of the shear layer development (x=2h), the turbulent energy of the baseline flow is small and the periodic behaviour of the shear layer is not installed at this location. At x=4h, the turbulent energy increases and it is dominated by a low frequency related to the flapping of the separated shear layer. However, small amplitudes peaks are also observed around 110 Hz (St_θ=0.011) and its subharmonics. Above the reattaching region, the flow organization is unchanged at the exception of the noticeable increase of the signature at the 110 Hz fundamental and its subharmonics. For the

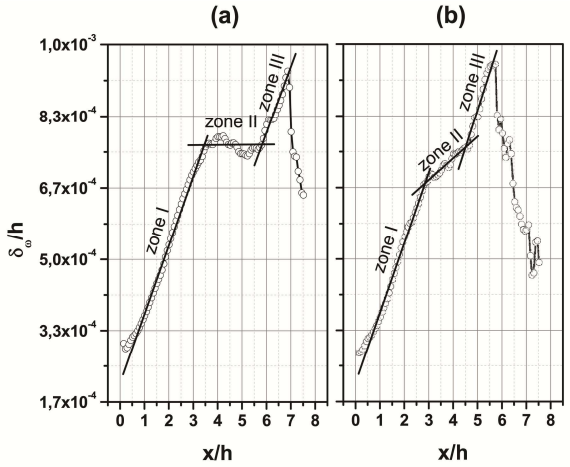

Figure 11: Evolution of the vorticity thickness along the free shear layer for natural (a) and flow controlled by optimized parameters (b).

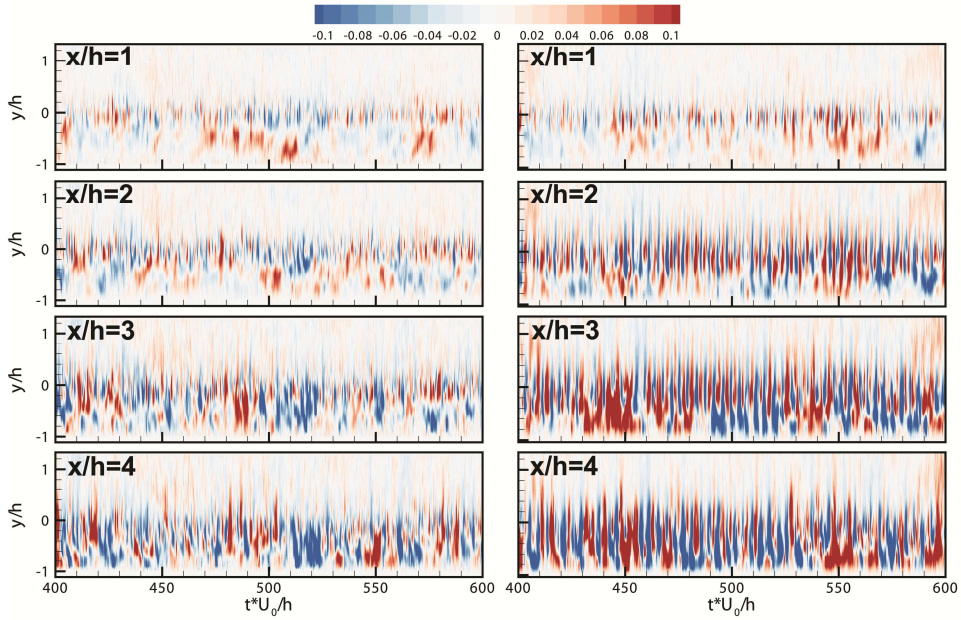

Figure 12: Time-history of the fluctuating velocity v' (normalized by U_0) at different x/h locations for the natural (left plot) and force flow (right plots)

actuation at the shear layer mode (125 Hz, St_θ=0.013), the influence of the actuator is clearly evidenced by the dominating peak observed at the forcing frequency this from the earlier stage of the vortex formation (x=2h). The shear layer oscillations are fully periodic. Later (x=4h), the peak at the forcing frequency is damped while the vortex pairing process becomes significant as demonstrated by the peaks at St_θ/2 and St_θ/4. After the reattachment point (x=6h), the frequency signature at St_θ=0.013 and its two first subharmonics emerge from the background turbulence, all of them having approximately similar amplitude. The presence of several quasi-discrete frequencies after the reattachment point shows that vortical flow structures persist beyond the reattachment point. These results demonstrate that the shear layer is dominated by a periodic phenomenon at a single frequency in the first stages of its development. At x=4h, the merging process of the vortical flow structures is already initiated. The single-frequency behaviour corresponds to zone I of the vorticity thickness while the vortical merging is observed in zone II. This further confirms that the optimized actuation produces a change in the shear layer development by enhancing the merging of the flow structures. The pairing process is known to enhance the regions of flow trapped between two successive vortical flow structures increasing further the transfer from the non-turbulent region to the recirculation zone [16]. So, the large reduction in the reattachment position derives from the increase in vortex pairing caused by the local forcing at the shear layer mode.

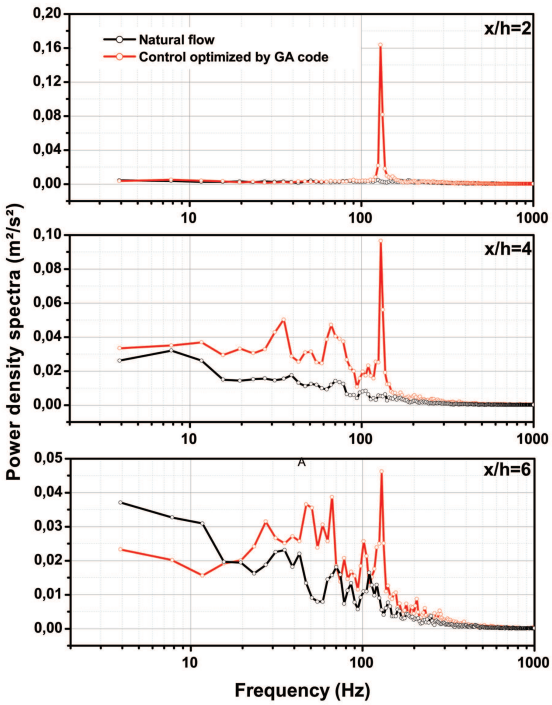

Figure 13: Power density spectra of the fluctuating velocity component v' for the natural flow and plasma optimized by GA code at different x/h locations.

5. CONCUSION

A multi-parameter flow control optimization by basic evolutionary algorithm has been conducted. To our knowledge, this research is the first

demonstration of an experiment coupled to numerical optimizer for flow control optimization. The genetic algorithm has confirmed its utility for optimizing several parameters in order to minimize a single objective function. The optimized forcing conditions significantly reduce the recirculation bubble and the conducted flow measurements confirm that the forcing conditions defined by the GA optimizer impacts the flow dynamic. In particular, a change in the growing of the shear layer has been demonstrated. The 2D linear periodic forcing by plasma actuator (tangential forcing) promotes vortex pairing and merging process, two mechanisms contributing to a shortened recirculation.

The use genetic algorithm to optimize single or multi-objective problems is of great interest for the flow control community, especially, where multiple or multi-frequency actuators are deployed individually, because new control mechanisms may be revealed. Furthermore, the research conducted here can be easily extended to more complex search space, other flow configuration or other type of flow control system.

6. ACKNOWLEDEGMENT

This work was funded by the 7th Framework program FP7/2010-2013, MARS (grant agreement n°266326).

7. REFERENCES

[1] L. Huang, G. Huang, R. LeBeau and T. Hauser, (2007) 'Optimization of airfoil flow control using a genetic algorithm with diversity control,' *J. Aircraft* **44**.

[2] A. Hilgers, and B.J. Boersma, (2001), 'Optimization of turbulent jet mixing,' *Fluid Dynamics Research* **29**, 345-368

[3] T.K. Sengupta, K. Deb, and S.B. Tala, (2007), 'Control of flow using genetic algorithm for a circular cylinder executing rotary oscillation,' *Computers and Fluids* **36**, 578-600

[4] T. Watanabe, T. Tatsukawa, A.L. Jaimes, H. Aono, T. Nonomura, A. Oyama, and K. Fujii, (2014), 'Many-objective evolutionary computation for optimization of separated-flow control using a DBD plasma actuator,' Evolutionary Computation (CEC) IEEE, 2849 – 2854.

[5] M.A.Z Hasan, (1992), 'The flow over a backward-facing step under controlled perturbation: laminar separation,' *J. Fluid Mechanics* **238**, 73-96

[6] N.J. Cherry, R. Hillier, and P. Latour, (1984), 'Unsteady measurements in a separated and reattaching flow', *J. Fluid Mechanics* **44**

[7] L.M. Hudy, A.M. Naguib, and W.M. Humphreys, (2003) 'Wall-pressure-array measurements beneath a separating / reattaching flow region', *Physics of Fluids* **15**

[8] N. Benard and E. Moreau, (2014), 'Electrical and mechanical characteristics of surface AC dielectric barrier discharge plasma actuators applied to airflow control,' *Experiments in Fluids* **55**

[9] J. d'Adamo, R. Sosa, and G. Artana, (2014), 'Active Control of a Backward Facing Step Flow With Plasma Actuators,' *Journal of Fluid Engineering* **136**

[10] N. Benard, P. Sujar-Garrido, K.D. Bayoda, J.P. Bonnet, and E. Moreau, (2014), 'Pulsed dielectric barrier discharge for manipulation of turbulent flow downstream a backward-facing-step,' AIAA paper 2014-1127

[11] S. Chun, Y.Z. Liu and H.J. Sung, (2004), 'Wall pressure fluctuations of a turbulent separated and reattaching flow affected by an unsteady wake,' *Experiments in Fluids* **37**, 531-546

[12] S. Bandyopadhyay and S. Saha, (2013), 'Unsupervised classification,' Springer-Verlag, 2013.

[13] J.F. Wang, J. Periaux, and M. Sefrioui, (2002), 'Parallel evolutionary algorithms for optimization problems in aerospace engineering,' *J. Comput. Appl. Math.* **149**, 155-169

[14] P. Sujar-Garrido, N. Benard, J.P. Bonnet and E. Moreau, (2015), 'Dielectric barrier discharge plasma actuator to control turbulent flow downstream of a backward-facing step 'To be published in *Experiments in Fluids*.

[15] K.B. Chun, and H.J. Sung, (1996), 'Control of turbulent separated flow over a backward-facing step by local forcing,' *Experiments in Fluids* **21**, 417-426.

[16] C.D. Winant, and F.K. Browand, (1974), 'Vortex pairing: the mechanism of turbulent layer growth at moderate Reynolds number,' *J. Fluid Mechanics* **63**, 237-255